1 **Stress-induced formation of cell wall-deficient cells in filamentous**

2 **actinomycetes**

3

4 K. Ramijan[1], E. Ultee[1], J. Willemse[1], A.J. Wondergem[2], D. Heinrich[2,3], A. Briegel[1], G.P. van

5 Wezel[1] and D. Claessen[1#]

6

7 [1]Molecular Biotechnology, Institute of Biology, Leiden University.

8 [2]Biological and Soft Matter Physics, Huygens-Kamerlingh Onnes Laboratory, Leiden

9 University

10 [3]Fraunhofer Institute for Silicate Research ISC, Würzburg, Germany

11

12

13

14 # To whom correspondence should be addressed

15 E-mail: D.Claessen@biology.leidenuniv.nl

16 Tel: +31 (0)71 527 5052

17

18 Keywords: hyperosmotic stress, morphogenesis, cell wall-deficient cells, S-cell, adaption

19

20

21

22

23

24

25

26

27

28 **ABSTRACT**

29 The cell wall is a shape-defining structure that envelopes almost all bacteria. One of its main

30 functions is to serve as a protection barrier to environmental stresses. Bacteria can be forced

31 in a cell wall-deficient state under highly specialized conditions, which are invariably aimed

32 at interrupting cell wall synthesis. Therefore, the relevance of such cells has remained

33 obscure. Here we show that many filamentous actinomycetes have a natural ability to

34 generate a new, cell wall-deficient cell type in response to hyperosmotic stress, which we call

35 S-cells. This wall-deficient state is transient, as S-cells are able to switch to the canonical

36 mycelial mode-of-growth. Remarkably, prolonged exposure of S-cells to hyperosmotic stress

37 yielded variants that are able to proliferate indefinitely without their cell wall. This is the

38 first report that demonstrates the formation of wall-deficient cells as a natural adaptation

39 strategy and their potential transition into stable wall-less forms solely caused by prolonged

40 exposure to osmotic stress. Given that actinomycetes are potent antibiotic producers, our

41 work also provides important insights into how biosynthetic gene clusters and resistance

42 determinants may disseminate into the environment.

43 **INTRODUCTION**

44 All free-living bacteria are challenged by constant changes in their environment, and their
45 survival depends on the ability to adapt to sudden exposure to stressful conditions. For
46 instance, soil bacteria can encounter rapid osmotic fluctuations caused by rain, flooding, or
47 desiccation. Bacterial cells typically respond to osmotic changes by rapidly modulating the
48 osmotic potential within the cell, either by importing or exporting ions and compatible
49 solutes[1]. While these responses typically occur immediately after cells have been exposed to
50 the changed environment, they are also able to tune the expression of metabolic pathways or
51 critical enzymes [2].

52 How such osmotic changes affect cellular morphology is not well known. The cells'
53 shape is largely dictated by the cell wall, which is a highly dynamic structure that acts as the
54 main barrier that provides osmotic protection [3]. The synthesis of its major constituent,
55 peptidoglycan (PG), involves the activity of large protein complexes that cooperatively build
56 and incorporate new PG precursors into the growing glycan strands at the cell surface [4-7].
57 These strands are then cross-linked to form a single, giant sacculus that envelops the cell [8].
58 The sites for the incorporation of new PG is a major difference between the planktonic
59 firmicutes that grow by extension of the lateral wall, and Actinobacteria, which grow via
60 apical extension and thereby incorporating new PG at the cell poles [9,10].

61 Actinobacteria display a wide diversity of morphologies, including cocci
62 (*Rhodococcus*), rods (*Mycobacterium* and *Corynebacterium*) and mycelia (*Streptomyces* and
63 *Kitasatospora*), or even multiple shapes (*Arthrobacter*)[11,12]. Species belonging to these
64 genera are able to change their morphology to adapt to extreme environments. For example,
65 *Rhodococcus* species that are commonly found in arid environments are able to adapt to
66 desiccation by modulating their lipid content and form short-fragmented cells [13].
67 *Arthrobacter* species also exhibit high resistance to desiccation and cold stresses. Upon
68 hyperosmotic stress, these cells can modulate the synthesis of osmoprotectants and switch
69 between rod-shaped and myceloid cells [12].

70 While the cell wall is considered an essential component of virtually all bacteria, most
71 species can be manipulated under laboratory conditions to produce so-called L-forms that are
72 able to propagate without their wall [14-17]. Typically, L-forms are generated by exposing
73 walled bacteria to high levels of lysozyme combined with antibiotics that target cell wall
74 synthesis in media containing high levels of osmolytes [18,19]. Stable L-forms that can
75 propagate indefinitely without the cell wall require two mutations that fall in separate classes

76   [18]. The first class of mutations leads to an increase in membrane synthesis, either directly by

77   increasing fatty acid biosynthesis, or indirectly by reducing cell wall synthesis [20]. The second

78   class of mutations reduces oxidative damage caused by reactive oxygen species, which are

79   detrimental to proliferation of L-forms [21]. Notably, proliferation of L-forms is independent of

80   the FtsZ-based division machinery [15,22]. Instead, their proliferation can be explained solely by

81   biophysical processes, in which an imbalance between the cell surface area to volume ratio

82   leads to spontaneous blebbing and the subsequent generation of progeny cells [20]. Such a

83   purely biophysical mechanism of L-form proliferation is not species-specific. This

84   observation has led to the hypothesis that early life forms propagated in a similar fashion well

85   before the cell wall had evolved [15,20,23]. Whether L-forms have functional relevance in

86   modern bacteria, however, is unclear.

87   Here we present evidence that many filamentous actinobacteria have a natural ability

88   to extrude cell wall-deficient (CWD) cells when exposed to high levels of osmolytes. These

89   newly-identified cells, which we call S-cells, synthesize PG precursors and are able to switch

90   to the canonical mycelial mode-of-growth. Remarkably, upon prolonged exposure to

91   hyperosmotic stress conditions, S-cells can acquire mutations that enable them to proliferate

92   in the CWD state as so-called S-forms, which are morphologically similar to L-forms but not

93   originating from walled cells exposed to cell wall-targeting agents. These results demonstrate

94   that the extrusion of S-cells and their transition into proliferating S-forms is a natural

95   adaptation strategy in filamentous actinobacteria, solely caused by prolonged exposure to

96   osmotic stress.

97

RESULTS

Hyperosmotic stress drives the formation of cell wall-deficient cells

100   Recent work suggests that hyperosmotic stress conditions affects apical growth in

101   streptomycetes [24]. Consistent with these observations, we noticed that growth was

102   progressively disturbed in the filamentous actinomycete *Kitasatospora viridifaciens*, when

103   increasing amounts of sucrose were added to the medium (Fig. 1A). In liquid cultures

104   containing more than 0.5 M sucrose, initiation of growth was delayed by at least 5 h

105   compared to media with low levels of sucrose. A similar retardation in growth was observed

106   on solid medium supplemented with high levels of osmolytes, evident from the size decrease

107   of colonies (Fig. 1B, C). On average, their size decreased from 12.8 mm^2 to 1.4 mm^2 after 7

108   days of growth. Notably, the high osmolarity also reduced the number of colony forming

109   units (CFU) by 33%, from 9.3×10^8 CFU ml^{-1} to 6.1×10^8 CFU ml^{-1}. In order to study the

110   morphological changes accompanying this growth reduction, we stained the mycelium after

111   48 h of growth with the membrane dye FM5-95 and the DNA stain SYTO-9 (Fig. 1D, E).

112   The high levels of osmolytes had a dramatic effect on mycelial morphology. The hyphae

113   showed indentations along the cylindrical part of the leading hyphae, reminiscent of initiation

114   of sporulation (see BF panel in Fig. 1E). In addition, the branching frequency increased by

115   more than three-fold in the presence of high levels of osmolytes (Extended Data Table 1 and

116   2, Student's T-test, *P*-value = 0,0010). Additionally, we noticed that these stressed hyphae

117   contained an excess of membrane (compare FM5-95 panels in Fig. 1D, E). The proportion of

118   the hyphae that were stained with FM5-95 increased from 10% to 21% in the presence of

119   0.64 M Sucrose (Extended Data Table 1 and 2, Student's T-test, *P*-value < 0,0001).

120   Simultaneously, the average surface area occupied by the nucleoid decreased from 2.59 µm^2

121   to 1.83 µm^2 (Extended Data Table 1 and 2, Student's T-test, *P*-value = 0.0074). Most

122   strikingly, we observed large DNA-containing vesicles surrounding the mycelial networks

123   (see arrowheads in Fig. 1E). High levels of NaCl had a similar effect on growth and

124   morphology (Fig. S1). *K. viridifaciens* was no longer able to grow when the NaCl

125   concentration was increased to more than 0.6 M (not shown). These results together indicate

126   that upon osmotic stress, the hyphae form a previously uncharacterized cell type, which we

127   hereinafter will refer to as S-cells, for stress-induced cells.

128   To distinguish S-cells from other cell wall-deficient (CWD) variants of *K.*

129   *viridifaciens*, we compared them to fresh protoplasts and L-form cells obtained after classical

130   induction with high levels of lysozyme and penicillin G (see Materials and Methods). Size

131   measurements from 2D images revealed that S-cells had an average surface area of 20.73

132   µm^2 and were considerably larger than protoplasts and L-forms, which had an average

133   surface area of 4.01 µm^2 and 7.06 µm^2, respectively. Vancomycin-BODIPY staining (van^{FL},

134   Fig. S2A) revealed a heterogeneous pattern of nascent PG synthesis in these cells, while in L-

135   forms mostly detached wall material was observed. By contrast, no staining was detected

136   when freshly prepared protoplasts were used (Fig. S2A). When protoplasts were maintained

137   in LPB for 48 hours, their average surface area increased to 7.49 ± 2.21µm^2, which is

138   considerably smaller than that of S-cells (Extended Data Table 3). Furthermore, protoplasts

139   regenerated a more uniform cell wall while S-cells showed a disordered, non-uniform pattern

140   of cell-wall assembly, whereby wall material was sometimes found to be detached from the

141   cell surface (Fig. S2B, Table Extended Data Table 3).

142

143 **Formation of S-cells is common in natural isolates**

144 To see how widespread the formation of S-cells is among natural isolates, we screened our

145 collection of filamentous actinomycetes, obtained from the Himalaya and Qinling mountains

146 [25], using *Streptomyces coelicolor*, *Streptomyces lividans*, *Streptomyces griseus*, and

147 *Streptomyces venezuelae* as the reference strains We used a cut-off diameter of 2 μm to

148 distinguish small S-cells from spores. Spherical cells, similar to S-cells were evident in

149 hyperosmotic media in *S. venezuelae* and in 7 out of the 96 wild isolates (Fig. S3A). The cells

150 were variable in size within the same strains and between strains (Fig. 2A, Extended Data

151 Table 4) and showed differences in the organization of their DNA (Fig. 2A). No S-cells were

152 found in *S. coelicolor, S. griseus,* or *S. lividans* under the tested conditions. Phylogenetic

153 analysis based on 16S rRNA (Fig. S3B), or the taxonomic marker gene *ssgB* used for

154 classifying morphologically complex actinomycetes [26] revealed that the formation of S-cells

155 is common in at least two genera (Fig. 2B). Moreover, the ability to form S-cells was not

156 restricted to strains that sporulate in liquid-grown cultures. This is based on the observation

157 that MBT86, which belongs to the *S. coelicolor* clade and is classified as a non-liquid

158 sporulating strain, also generates S-cells (Fig. 2C). Altogether, these results show the natural

159 ability to generate S-cells is widespread in filamentous actinomycetes.

160

161 **S-cells are viable cells with the ability to switch to the mycelial mode-of-growth**

162 To determine where S-cells are generated in the hyphae, we performed live imaging of

163 growing germlings of *K. viridifaciens* (Extended Data Video S1). Approximately 7 h after the

164 visible emergence of germ tubes, we detected a transient arrest in tip extension of the leading

165 hypha (Fig. 3A, t=400 mins). Shortly thereafter, small S-cells became visible, which were

166 extruded from the hyphal tip (see arrows in Fig. 3A). These cells rapidly increased in size and

167 number. After 545 min a narrow branch (Fig. 3A arrowhead) was formed in the apical region

168 from which the S-cells were initially extruded. Subapically, other branches became visible

169 approximately 210 minutes after the first appearance of these cells (Extended Data Video S1,

170 t= 770 min). Notably, such branches frequently also extruded S-cells, similarly to the leading

171 hypha (Extended Data Video S2). This showed that S-cells are produced at hyphal tips after

172 apical growth was arrested.

173 Further characterization of S-cells from *K. viridifaciens* revealed that these cells had a

174 granular appearance and membrane assemblies that stained with FM5-95 (Fig. 3B, arrows,

175 Supplementary Video S3). Notably, these assemblies often co-localized with DNA (Fig. 3B,

176 arrows). To study S-cells in more detail, we separated them after 7 days from the mycelia by

177   filtration (see Materials and Methods). In agreement with the previous findings, we also

178   detected agglomerates of membrane assemblies in close proximity of the DNA using electron

179   microscopy analysis (Fig. 3C). Additionally, we noticed that S-cells possessed a disorganized

180   surface, characterized by membrane protrusions that appeared to detach from the S-cells (Fig.

181   3D, 3E), and an apparent deficiency in normal cell-wall biogenesis (compare to the cell

182   surface of the hypha in Figs. 3F, 3G).

183   To establish if S-cells were truly viable cells, they were plated onto plates

184   supplemented with sucrose. After 7 days of growth, many mycelial colonies were found;

185   demonstrating that the cells indeed were viable, and that such cell are only transiently CWD

186   (Fig. 3H; ± 1.6x10^4 CFUs ml^{-1} of the filtered culture). Time-lapse microscopy (Extended

187   Data Video S4) revealed that the cells (Fig. 3I, asterisk) initiated filamentous growth and

188   established mycelial colonies, which, in turn, also extruded new S-cells from the hyphal tips

189   (Fig. 3I, arrowheads). A switch to mycelial growth was also observed when S-cells were

190   inoculated in liquid medium, whether or not the media was supplemented with high levels of

191   sucrose (data not shown). We noticed that the viability of S-cells was reduced by 60%

192   (decreasing from 1.6x10^4 to 6.7 x10^3 CFUs ml^{-1}) when these cells were diluted in water

193   before plating. Microscopy analysis indicated that the surviving S-cells were those that

194   showed abundant staining with WGA-Oregon (Fig. S4). Altogether, these results demonstrate

195   that *K. viridifaciens* generates S-cells that synthesize PG and are able to switch to the

196   mycelial mode-of-growth.

197

198   **S-cell formation frequently leads to loss of the linear megaplasmid KVP1**

199   When S-cells were allowed to switch to mycelium on MYM medium, we identified many

200   colonies with developmental defects (Fig. 4A). Most obvious was the frequent occurrence of

201   small, brown-colored colonies that failed to produce the white aerial hyphae or the grey-

202   pigmented spores. Non-differentiating colonies are referred to as bald, for the lack of the

203   fluffy aerial hyphae [27]. To test if this aberrant phenotype was maintained in subsequent

204   generations, we selected three of these bald colonies (R3-R5) and two grey-pigmented

205   colonies with a near wild-type morphology (R1 and R2) for further analysis. The progeny of

206   the grey colonies developed similarly to the wild-type strain, and sporulated abundantly after

207   7 days of growth (Fig. 4B). In contrast, strains R3-R5 failed to sporulate after 7 days of

208   growth. This phenotype is reminiscent of the defective sporulation seen in colonies of

209   *Streptomyces clavuligerus* that have lost the large linear plasmid pSCL4 following protoplast

210   formation and regeneration[28]. Given that *K. viridifaciens* contains a large megaplasmid

211   (KVP1 [29]), we reasoned that S-cell formation could increase the frequency of the loss of this

212   plasmid. To test this assumption, we performed quantitative real-time PCR using four genes

213   contained on the megaplasmid (*orf1, parA, tetR,* and *allC*). As a control, we included the two

214   house-keeping genes *infB* and *atpD,* both of which are located on the chromosome, and

215   which encode the translation initiation factor IF-2 and a subunit of the F_0F_1 ATP synthase,

216   respectively. Detectable amplification of *infB* and *atpD* was seen after 19 PCR cycles in

217   strains R3-R5, which was similar to the wild-type strain (Fig. 4C). The same was true for the

218   KVP1-specific genes *orf1, parA, tetR,* and *allC* in the wild-type strains. However,

219   amplification of these plasmid marker genes was only seen after 30 PCR cycles in strain R3-

220   R5 (Fig. 4D). This demonstrates that the KVP1-specific genes were only present in trace

221   amounts in the R3-R5 strains (at least 10^4 times less abundant than the chromosomal genes

222   *infB* and *atpD*) (Fig. 4E), which is consistent with loss of KVP1 during formation of S-cells.

223

224   **Prolonged hyperosmotic stress is sufficient to convert S-cells into proliferating S-forms**

225   Although the switch to mycelial growth was exclusively observed when young S-cells were

226   cultured in fresh media, we noticed a dramatic change when S-cells had been exposed for

227   prolonged periods to the hyperosmotic stress conditions. In nine out of 15 independent

228   experiments, we found that S-cells switched to mycelial growth, while four times S-cells

229   failed to form a growing culture. Strikingly, however, were the two independent occasions

230   during which S-cells had proliferated in an apparent cell wall-deficient state. On solid

231   medium, these two independent cell lines, called M1 and M2 (for mutants 1 and 2,

232   respectively, see below), formed viscous colonies on LPMA medium, which were similar to

233   those formed by the L-form lineage induced with penicillin and lysozyme, but distinct from

234   the compact colonies formed by the wild-type strain (Fig. 5A). Liquid-grown cultures of M1

235   and M2 exclusively consisted of CWD cells when sucrose and $MgCl_2$ were added (Fig. 5B,

236   BF panels). Staining with WGA-Oregon Green showed these cell lines were indeed cell wall-

237   deficient, as nascent peptidoglycan was mainly found detached from the cell surface (Fig.

238   S5). The spherical cells produced by M1 and M2 were comparable in size to the PenG-

239   induced L-forms. Further microscopic analysis revealed that the cells from M1 and M2

240   contained inner vesicles (arrowheads in Fig 5B) and tubular protrusions emerging from the

241   cell surface (Fig. 5B, inlay). The vast majority of cells contained DNA, although some empty

242   vesicles were also evident in M1 and M2 (Fig. 5B, asterisks). Time-lapse microscopy

243   revealed that both strains proliferated, whereby smaller progeny cells were released following

244   deformation of the mother cell membrane by either vesiculation (Fig. 5C, taken from

245   Extended Data Video S5), blebbing (Fig. 5D, taken from Extended Data Video S6) or

246   tubulation (Fig. 5E, taken from Extended Data Video S7). Altogether these results inferred

247   that strains M1 and M2 closely resemble the previously described L-forms, both in the

248   inability to regain a cell wall as well as the ability to proliferate in the cell-wall-less state.

249   However, instead of originating from prolonged exposure to antibiotic and/or lysozyme

250   treatment, they originate from osmotically stress-induced cells, and we therefore will call

251   these cells S-forms.

252   The low frequency at which S-form cells formed made us wonder whether M1 and

253   M2 had acquired mutations that enabled these strains to proliferate without a proper cell wall.

254   Real-time qPCR studies revealed that M1 and M2, but also the PenG-induced L-form cell

255   line, had lost the megaplasmid (Fig. S6). However, loss of the megaplasmid is not sufficient

256   to drive the transition from S-cells to S-forms, as strains R3-R5, all of which had lost the

257   KVP1 megaplasmid, formed mycelia extruding S-cells under hyperosmotic stress conditions

258   (data not shown). Single nucleotide polymorphism (SNP) analysis following whole genome

259   sequencing showed that M1 and M2 had acquired several other mutations (Extended table 5

260   and 6). Interestingly, both strains carried a mutation in the gene BOQ63_RS21920, which

261   encodes a putative metal ABC transporter. Transporters are often used to cope with osmotic

262   stress conditions [30]. We also identified mutations in the PenG-induced L-form strain

263   (Extended table 7). These mutations, however, differed from those observed in the S-form

264   strains M1 and M2. Notably, the mutations in the PenG-induced L-form appeared to directly

265   relate to cell wall biogenesis, for example in the case of the mutation in *uppP*. The encoded

266   protein is involved in the recycling pathway of the carrier lipid undecaprenyl phosphate

267   (BOQ63_RS22750), which transports glycan biosynthetic intermediates for cell wall

268   synthesis. Altogether, these results demonstrate that prolonged exposures to hyperosmotic

269   stress conditions are apparently sufficient to convert a bacterium into an S-form strain that

270   proliferates without the cell wall.

271

272   **DISCUSSION**

273   Filamentous actinomycetes have been intensely studied for more than 50 years as a model for

274   bacterial development. Here, we provide compelling evidence that S-cells represent a natural

275   and previously unnoticed developmental stage in these organisms when they are exposed to

276   hyperosmotic stress conditions (Fig. 5F). These S-cells are extruded from the hyphal tips,

277   they contain DNA and are viable with the ability to grow into mycelial colonies.

278   Furthermore, upon prolonged exposure to hyperosmotic stress, S-cells may also accumulate

279   mutations that enable them to efficiently proliferate in the wall-deficient state we have

280   dubbed S-forms. Our data show that these S-forms can simply emerge as the product of

281   prolonged exposure of cells to hyperosmotic conditions, without directly requiring cell wall-

282   targeting agents. This work provides compelling evidence that such cells have an ecological

283   relevance.

284   Environmental fluctuations can dramatically influence the availability of water in

285   ecosystems and present osmotic shock conditions to organisms. For instance, microorganisms

286   living in hyperarid regions or hypersaline aquatic environments are frequently exposed to

287   desiccation or hypertonicity [31]. Also, microbes in snow and ice habitats experience low water

288   availability and hypersaline or hyper-acidic environments [32]. Bacteria can adapt to these

289   fluctuations by modulating fatty acid synthesis, accumulating or synthesizing

290   osmoprotectants, protecting their DNA, and secreting extracellular polymeric substance [31,33].

291   Here, we focused on the adaptation of filamentous actinomycetes, which are common

292   in any soil, to extended periods of hyperosmotic stress. As expected, we detected that these

293   bacteria increased the amount of membrane in the hyphae and condensed their nucleoids.

294   Surprisingly though was the extrusion of S-cells. Together with sporulation and the recently

295   discovered explorative mode-of-growth [34], the ability to form S-cells extends the repertoire

296   by which filamentous actinomycetes can thrive in changing environments. In addition to

297   switching to mycelial growth, these S-cells can have multiple fates. As these cells are wall-

298   deficient, they are prone to lysis due to influx of water. Indeed, exposure to water leads to a

299   steep decline in their ability to outgrow into colonies. However, even when S-cells lyse, the

300   DNA cargo will be released into the environment. Given the large number of biosynthetic

301   gene clusters (BGCs) that are present in the genomes of filamentous actinomycetes, including

302   their resistance determinants, this release of DNA may be a significant, and previously

303   unknown mechanism by which resistance genes are spread. In contrast to releasing DNA into

304   the environment, the S-cells may be able to take up DNA from the environment, similar to

305   other cell wall-deficient cell types such as protoplasts or L-forms [35]. This would enable the

306   cells to acquire genetic information that may help them to overcome the stressful conditions

307   to which they are exposed. In other organisms, this concept has been well characterized. For

308   instance, the bacterium *Bacillus subtilis* becomes naturally competent towards the end of the

309   exponential growth phase [36]. This allows the cells to pick up DNA from the environment,

310   with the prospect of withstanding the harsh conditions and improving the likelihood of

311   survival. Likewise, competence of *Streptococcus pneumoniae* is promoted by exposure to

312   antibiotics that target DNA replication [37]. This, in turn, enables the uptake of foreign DNA

313   (e.g. genes conferring antibiotic resistance). As such, maximizing survival by DNA uptake is

314   a proven strategy.

315   Our work shows that S-cells are extruded from hyphal tips into the environment,

316   coinciding with an arrest in tip growth. Following their release, the extruding hypha

317   reinitiates growth, indicating that the extrusion process occurs in a manner that apparently is

318   not lethal for the filament from which the cells are released. Tip growth in filamentous

319   actinomycetes is coordinated by the polarisome complex, of which the DivIVA protein is a

320   crucial member [38]. Recent work revealed that hyperosmotic stress has a dramatic effect on the

321   polar growth machinery. Following osmotic upshift experiments, tip growth is arrested,

322   followed by relocation of the apical growth machinery to subapical sites. As a consequence,

323   lateral branches emerge from the leading hyphae [24]. We hypothesize that an imbalance

324   between cell wall synthesis and cell wall turnover could locally lead to changes in the

325   thickness or structure of the cell wall, allowing S-cells to escape from the sacculus.

326

327   **Hyperosmotic stress-induced formation of S-forms**

328   L-forms have been studied for many decades, and only recently are we beginning to

329   understand their exciting biology, especially due to ground-breaking work from the Errington

330   lab. L-form cells have been artificially generated from many different bacteria in many

331   laboratories, invariably aimed at targeting the biosynthesis pathway of the cell wall. To that

332   end, cells are typically exposed to high levels of antibiotics, either or not combined with

333   lysozyme treatment [18,23]. Our work expands on this research by providing for the first-time

334   evidence that CWD strains can emerge solely by exposure to hyperosmotic stress conditions

335   and implies an environmental relevance of this cell type. A crucial and limiting step in the

336   formation of L-forms in *B. subtilis*, as well as in other bacteria, is the escape of a protoplast

337   from the cell-wall sacculus. This process requires lytic activity, which usually comes from

338   lysozyme activity [39]. Our data show that actinomycetes have a natural ability to release such

339   CWD cells when exposed to hyperosmotic conditions. Under prolonged exposure to osmotic

340   stress, some cells are able to acquire mutations allowing these cells to propagate as S-forms.

341   In line with these findings, recent work shows that *B. subtilis* and *S. aureus* both are able to

342   convert to wall-deficient cells. This has been shown in an animal infection model as well as

343   in macrophages, where lysozyme activity from the host converts walled bacteria into CWD

344   cells [39]. Collectively, these results indicate that cell wall-deficient cells represent an adaptive

345   morphology allowing cells to overcome environmental challenges, such as antibiotic

346   treatment or hyperosmotic stress conditions.

347   In summary, our work provides evidence for a new, cell wall-deficient cell type in the

348   biology of filamentous actinomycetes. It further expands the large diversity in bacterial cell

349   types, and the plasticity that microorganisms employ to handle environmental stresses. It

350   remains to be elucidated how the ability to form S-cells improves fitness in these filamentous

351   actinomycetes, and how this morphogenetic switch is regulated.

352

353   **MATERIALS AND METHODS**

354   **Strains and media**

355   Bacterial strains used in this study are shown in Extended Data Table 8. To obtain

356   sporulating cultures, *Streptomyces* and *Kitasatospora* species were grown at 30°C for 4 days

357   on MYM medium [40]. To support growth of CWD cells, strains were grown on solid medium

358   L-Phase Medium (LPMA), containing 0.5% glucose, 0.5% yeast extract, 0.5% peptone, 20%

359   sucrose, 0.01% $MgSO_4 \cdot 7H_2O$, 0.75% Iberian agar (all w/v). After autoclaving, the medium

360   was supplemented with $MgCl_2$ (final concentration of 25 mM) and 5% (v/v) horse serum.

361   L-Phase Broth (LPB) was used as liquid medium to support growth of wall-deficient

362   cells. LPB contains 0.15% yeast extract, 0.25% bacto-peptone, 0.15% oxoid malt extract,

363   0.5% glucose, 0.64 M sucrose, 1.5% oxoid tryptic soy broth powder (all w/v) and 25 mM

364        $MgCl_2$. To test the effect of different sucrose concentrations on mycelial growth and the

365   formation of S-cells, the amount of sucrose in LPB was changed to obtain final

366   concentrations of 0.0, 0.12, 0.18, 0.50 and 0.64 M. The influence of sodium chloride as an

367   osmolyte was analysed by replacing sucrose with NaCl. 50 ml cultures were inoculated with

368   10^6 spores ml^{-1} and grown in 250 ml flasks. Cultures were incubated at 30°C, while shaking

369   at 100 rpm.

370   To prepare protoplasts of *K. viridifaciens*, the wild-type strain was grown for 48 hours

371   in a mixture of TSBS and YEME (1:1 v/v) supplemented with 5 mM $MgCl_2$ and 0.5%

372   glycine. Protoplasts were prepared as described [41], with the difference that 10 mg ml^{-1}

373   lysozyme solution was used for three hours. Freshly-made protoplast were diluted and

374   immediately used for fluorescence microscopy.

375

376   **Optical density measurements**

377   The growth of *K. viridifaciens* was monitored with the Bioscreen C reader system (Oy

378   Growth Curves AB Ltd). To this end, aliquots of 100 µl of LPB medium with different

379   concentrations of sucrose were added to each well of the honeycomb microplate and

380   inoculated with 10^6 spores ml^{-1}. Growth was monitored for 24 hours at 30°C, while shaking

381   continuously at medium speed. The OD wide band was measured every 30 min and corrected

382   for the absorbance of liquid medium without inoculum. In total, five replicate cultures were

383   used for each osmolyte concentration. The effect of sodium chloride as osmolyte was tested

384   using the same procedure, with the differences that the final volume of the cultures was 300

385   μl, and the experiment was run for 96 hours.

386

387   **Quantification of the number and size of colonies**

388   Serial dilutions of *K. viridifaciens* spores were plated in triplicates in LPMA (high

389   osmolarity) and LPMA without sucrose, $MgCl_2$ and horse serum (low osmolarity). After 7

390   days of incubation at 30°C the number of colonies was counted to determine the CFU ml^{-1}.

391   Quantification of the surface area of colonies was done with FIJI [42].

392

393   **Screening for strains with the ability to release S-cells**

394   To identify strains that are able to release S-cells, strains from an in-house culture collection

395   [25] were initially grown in flat-bottom polysterene 96-well plates, of which each well

396   contained 200 μl LPB medium and 5 μl of spores. The 96-well plate was sealed with parafilm

397   and incubated at 30°C for 7 days. The cultures were then analysed with light microscopy, and

398   strains with the ability to release S-cells with a diameter larger 2 μm were selected. The

399   selected strains were then grown in 250 mL flasks containing 50 mL LPB medium (10^6

400   spores ml^{-1}) at 30°C while shaking at 100 rpm. After 7 days, aliquots of 50 μl of the bacterial

401   cultures were fluorescently stained with SYTO-9 and FM5-95. The surface area of the S-cells

402   was determined in FIJI [42]. Assuming circularity of these cells, the corresponding diameter D

403   was then calculated as

404   D = 2 * [SQRT(area/π)].

405

406   **Filtration of S-cells from *K. viridifaciens***

407   50 ml LPB cultures of *K. viridifaciens*, inoculated with 10^6 spores ml^{-1}, were grown for 2 or 7

408   days at 30°C in an orbital shaker at 100 rpm. To separate the S-cells from the mycelium, the

409   cultures were passed through a sterile filter made from an EcoCloth™ wiper. A subsequent

410   filtration step was done by passing the S-cells through a 5 μm Isopore™ membrane filter.

411   The filtered vesicles were centrifuged at 1,000 rpm for 40 mins, after which the supernatant

412   was carefully removed with a 10 mL pipette to avoid disturbance of the S-cells.

413

414

Viability and subculturing of S-cells from *K. viridifaciens*

To verify the viability of S-cells, the filtered cells were incubated in 10 mg ml^{-1} lysozyme solution for 3 hours at 30°C, while shaking at 100 rpm to remove residual hyphal fragments. The filtered S-cells were then centrifuged at 1,000 rpm for 40 mins and resuspended in 1 volume of fresh LPB. Serial dilutions of the S-cells in LPB or water were then plated, in triplicate, on LPMA or MYM medium. The plates were grown for 7 days at 30°C and the CFU values were determined for each treatment.

Generation of the PenG-induced L-form cell line

Generation of the *K. viridifaciens* L-form lineage was performed by inoculating the wild-type strain in 50 mL LPB medium, supplemented with lysozyme and/or penicillin G, in 250 mL flasks in an orbital shaker at 100 rpm. Every week, 1 mL of this culture was transferred to fresh LPB medium according to the cultivation regime previously described [19]. After the 8th subculture, the inducers were removed from the cultivation medium and the obtained lineage did not revert back to the walled state on LPMA plates or in LPB medium. A single colony obtained after the 8th subculture was designated as PenG-induced L-forms.

Phylogenetic analysis

The 16S rRNA sequences from strains of the in-house culture collection were previously determined [25]. Homologues of *ssgB* in these strains were identified by BLAST analysis using the *ssgB* sequence from *S. coelicolor* (SCO1541) as the input. For the *Streptomyces* and *Kitasatospora* strains whose genome sequence was not available, the *ssgB* sequence was obtained by PCR with the *ssgB* consensus primers (Extended Data Table 9). Geneious 9.1.7 was used to make alignments of *ssgB* and 16S rRNA, and for constructing neighbour-joining trees.

Quantitative real time PCR

Filtered S-cells were allowed to regenerate on MYM medium, from which three regenerated bald colonies (R3, R4, and R5) were selected. After two rounds of growth on MYM, bald colonies of the three strains were grown in TSBS for 2 days at 30°C, and genomic DNA was isolated from these strains as described [41]. Primers were designed to amplify the *infB* (BOQ63_RS18295) and *atpD* (BOQ63_RS18295) genes located in the chromosome, and four genes located on the KVP1 megaplasmid: *allC* (BOQ63_RS01235), *tetR* (BOQ63_RS09230), *parA* (BOQ63_RS03875) and *orf1* (BOQ63_RS04285) (Extended Data

449   Table 9). The PCR reactions were performed in triplicate in accordance with the

450   manufacturer's instructions, using 5 ng of DNA, 5% DMSO and the iTaq Universal SYBR

451   Green Supermix Mix (Bio-Rad). Quantitative real time PCR was performed using a CFX96

452   Touch Real-Time PCR Detection System (Bio-Rad). To normalize the relative amount of

453   DNA, the wild-type strain was used as a control, using the *atpD* gene as a reference.

454

455   **Isolation of the hyperosmotic stress-induced S-form cell lines M1 and M2**

456   Fifteen replicate cultures of *K. viridifaciens* were grown for 7 days in LPB medium. After

457   filtration, the S-cells were transferred to fresh LPB medium. The cultures that had not

458   switched to mycelium after 3 days of cultivation were kept for further analysis. Two cultures

459   turned dark green after 7 days, which after inspection with light microscopy contained

460   proliferating S-form cells. These cell lines were named M1 and M2.

461

462   **Microscopy**

463   Bright field images were taken with the Zeiss Axio Lab A1 upright Microscope, equipped

464   with an Axiocam MRc with a resolution of 64.5 nm/pixel.

465

466   *Fluorescence microscopy*

467   Fluorescent dyes (Molecular Probes[TM]) were added directly to 100 µl aliquots of liquid-

468   grown cultures. For visualization of membranes, FM5-95 was used at a final concentration of

469   0.02 mg ml^{-1}. Nucleic acids were stained with 0.5 µM of SYTO-9 or 0.05 mg ml^{-1} of Hoechst

470   34580. The detection of nascent peptidoglycan was done using 0.02 mg ml^{-1} Wheat Germ

471   Agglutinin (WGA) Oregon Green, or 1 µg ml^{-1} BOPIPY FL vancomycin. Prior to

472   visualization, cells and mycelium were applied on a thin layer of LPMA (without horse

473   serum) covering the glass slides. Confocal microscopy was performed using a Zeiss Axio

474   Imager M1 Microscope. Samples were excited using a 488-nm laser, and fluorescence

475   emissions for SYTO-9, and WGA Oregon Green were monitored in the region between 505–

476   600 nm, while a 560 nm long pass filter was used to detect FM5-95. Detailed fluorescence

477   microscopy pictures (i.e. those in Figures 1D-E, S1C-D, 5B) represent average Z-projections

478   of stacks.

479   The characterization of the membrane assemblies in S-cells was done on a Nikon

480   Eclipse Ti-E inverted microscope equipped with a confocal spinning disk unit (CSU-X1)

481   operated at 10,000 rpm (Yokogawa, Japan) using a 100x Plan Fluor Lens (Nikon, Japan) and

482   illuminated in bright-field and fluorescence. Samples were excited at wavelengths of 405 nm

483   and 561 nm for Hoechst and FM5-95, respectively. Fluorescence images were created with a

484   435 nm long pass filter for Hoechst, and 590-650 nm band pass for FM5-95. Z-stacks shown

485   in Extended Data Video S3 were acquired at 0.2 µm intervals using a NI-DAQ controlled

486   Piezo element.

487   Visualization of stained CWD cells for size measurements were done using the Zeiss

488   Axio Observer Z1 microscope. Aliquots of 100 µl of stained cells were deposited in each

489   well of the ibiTreat µ-slide chamber (ibidi®). Samples were excited with laser light at

490   wavelengths of 488, the green fluorescence (SYTO-9, BODIPY FL vancomycin, WGA-

491   Oregon) images were created with the 505-550 nm band pass, while a 650 nm long pass filter

492   was used to detect FM-595. An average Z-stack projection was used to make Fig. S2A.

493

494   *Time-lapse microscopy*

495   To visualize the emergence of S-cells, spores of *K. viridifaciens* were pre-germinated in

496   TSBS medium for 5 hours. An aliquot of 10 µl of the recovered germlings was placed on the

497   bottom of an ibiTreat 35 mm low imaging dish (ibidi®), after which an LPMA patch was

498   placed on top of the germlings.

499   To visualize switching of S-cells, these cells were collected after 7 days by filtration

500   from a *K. viridifaciens* LPB liquid-grown culture. A 50 µl aliquot of the filtrate was placed

501   on the bottom of an ibiTreat 35 mm low imaging dish (ibidi®) with a patch of LPMA on top.

502   To visualize the proliferation of M1 and M2, the strains were grown for 48 hours in

503   LPB. Aliquots of the culture were collected, and centrifuged at 9,000 rpm for 1 min, after

504   which the supernatant was removed, and the cells resuspended in fresh LPB. Serial dilutions

505   of the cells were placed in wells of a ibiTreat µ-slide chamber (ibidi®).

506   All samples were imaged for ~15 hours using an inverted Zeiss Axio Observer Z1

507   microscope equipped with a Temp Module S (PECON) stage-top set to 30°C. Z-stacks with a

508   1 µm spacing were taken every five minutes using a 40x water immersion objective. Average

509   intensity projections of the in-focus frames were used to compile the final movies. Light

510   intensity over time was equalised using the correct bleach plugin of FIJI.

511

512   *Electron microscopy*

513   To visualize the vegetative mycelium of *K. viridifaciens* by transmission electron microscopy

514   (TEM), the strain was grown in TSBS medium for 48 hours. An aliquot of 1.5 ml of the

515   cultures was centrifuged for 10 mins at 1,000 rpm, after which the supernatant was carefully

516   removed with a pipette. The mycelium was washed with 1X PBS prior to fixation with 1.5%

517   glutaraldehyde for one hour at room temperature. The fixed mycelium was centrifuged with

518   2% low melting point agarose. The solid agarose containing the embedded mycelium was

519   sectioned in 1 mm^3 blocks, which were post-fixed with 1% osmium tetroxide for one hour.

520   The samples were then dehydrated by passing through an ethanol gradient (70%, 80%, 90%

521   and 100%, 15 min per step). After incubation in 100% ethanol, samples were replaced in

522   propylene oxide for 15 minutes followed by incubation in a mixture of Epon and propylene

523   oxide (1:1) and pure Epon (each step one hour). Finally, the samples were embedded in Epon

524   and sectioned into 70 nm slices, which were placed on 200-mesh copper grids. Samples were

525   stained using uranyl-430 acetate (2%) and lead-citrate (0.4%), if necessary, and imaged at 70

526   kV in a Jeol 1010 transmission electron microscope.

527   To image S-cells, a culture of the wild-type *K.viridifaciens* strain that had been grown

528   in LPB medium for 7 days was immediately fixed for one hour with 1.5% glutaraldehyde.

529   Filtered S-cells (see above) were then washed twice with 1X PBS prior to embedding in 2%

530   low melting agarose. A post-fixation step with 1% OsO4 was performed before samples were

531   embedded in Epon and sectioned into 70 nm slices (as described above). Samples were

532   stained using uranyl-430 acetate (2%) and lead-citrate (0.4%), if necessary, and imaged at 70

533   kV in a Jeol 1010 transmission electron microscope

534

535   *Image analysis*

536   Image analysis was performed using the FIJI software package. To describe the

537   morphological changes during hyperosmotic stress, we compared mycelium grown in LPB

538   with or without 0.64 M of sucrose (i.e. the concentration in LPB medium). After making

539   average Z-stack projections from mycelia, 10 hyphae derived from independent mycelia

540   projections were further analysed. For each hypha, the total length was measured using the

541   segmented line tool and the number of branches emerging from that hypha was counted. The

542   hyphal branching ratio was calculated as the number of branches per μm of leading hypha.

543   To calculate the surface area occupied by membrane in hyphae either or not exposed

544   to 0.64 M sucrose, we divided the total surface area that stained with FM5-95 by the total

545   surface area of the hypha. FIJI was also used to measure the average surface area of the

546   nucleoid (using SYTO-9 staining) in both growth conditions. Student's T-tests with two-

547   sample unequal variance were performed to calculate *P*-values and to discriminate between

548   the samples.

549   To determine the size of cell wall-deficient (CWD) cells, we compared cells of PenG-

550   induced L-form to fresh protoplasts and S-cells, all obtained or prepared after 48 hours of

551   growth. Cells were stained with FM5-95 and SYTO-9 and deposited in the wells of an

552   ibiTreat µ-slide chamber (ibidi®). The size of the spherical was determined as the surface

553   area enclosed by the FM5-95-stained membrane. For the particular case of L-forms, where

554   empty vesicles are frequent, only cells that contained DNA were measured. At least 200 cells

555   of each CWD variant were analysed. Proliferating L-forms in which the mother cell could not

556   be separated from the progeny, were counted as one cell.

557

558   Genome sequencing and SNP analysis

559   Whole-genome sequencing followed by *de novo* assembly (Illumina and PacBio) and variant

560   calling analyses were performed by BaseClear (Leiden, The Netherlands). The unique

561   mutations were identified by direct comparison to the parental strain *Kitasatospora*

562   *viridifaciens* DSM40239 (GenBank accession number PRJNA353578 [29]). The single and

563   multiple nucleotide variations were identified using a minimum sequencing coverage of 50

564   and a variant frequency of 70%. To reduce the false positives the initial variation list was

565   filtered, and the genes with unique mutations were further analysed. All variants were

566   verified by sequencing PCR fragments (primer sequence in Extended table S9).

567

568

569

REFERENCES

1   Sleator, R. D. & Hill, C. Bacterial osmoadaptation: the role of osmolytes in bacterial stress and virulence. *FEMS Microbiol. Rev.* **26**, 49-71 (2002).

2   Poolman, B., Spitzer, J. J. & Wood, J. M. Bacterial osmosensing: roles of membrane structure and electrostatics in lipid–protein and protein–protein interactions. *Biochim. Biophys. Acta* **1666**, 88-104, doi:https://doi.org/10.1016/j.bbamem.2004.06.013 (2004).

3   Kysela, D. T., Randich, A. M., Caccamo, P. D. & Brun, Y. V. Diversity takes shape: understanding the mechanistic and adaptive basis of bacterial morphology. *PLoS Biol.* **14**, e1002565, doi:10.1371/journal.pbio.1002565 (2016).

4   Typas, A., Banzhaf, M., Gross, C. A. & Vollmer, W. From the regulation of peptidoglycan synthesis to bacterial growth and morphology. *Nat. Rev. Microbiol.* **10**, 123-136, doi:10.1038/nrmicro2677 (2012).

5   Meeske, A. J. *et al.* SEDS proteins are a widespread family of bacterial cell wall polymerases. *Nature* **537**, 634-638, doi:10.1038/nature19331 (2016).

6   Szwedziak, P. & Löwe, J. Do the divisome and elongasome share a common evolutionary past? *Curr. Opin. Microbiol.* **16**, 745-751, doi:10.1016/j.mib.2013.09.003 (2013).

7   Claessen, D. *et al.* Control of the cell elongation-division cycle by shuttling of PBP1 protein in *Bacillus subtilis*. *Mol. Microbiol.* **68**, 1029-1046, doi:10.1111/j.1365-2958.2008.06210.x (2008).

8   Höltje, J. V. Growth of the stress-bearing and shape-maintaining murein sacculus of *Escherichia coli*. *Microbiol. Mol. Biol. Rev.* **62**, 181-203 (1998).

9   Flärdh, K. & Buttner, M. J. *Streptomyces* morphogenetics: dissecting differentiation in a filamentous bacterium. *Nat. Rev. Microbiol.* **7**, 36-49, doi:10.1038/nrmicro1968 (2009).

10   Claessen, D., Rozen, D. E., Kuipers, O. P., Søgaard-Andersen, L. & van Wezel, G. P. Bacterial solutions to multicellularity: a tale of biofilms, filaments and fruiting bodies. *Nat. Rev. Microbiol.* **12**, 115-124, doi:10.1038/nrmicro3178 (2014).

11   Barka, E. A. *et al.* Taxonomy, physiology, and natural products of *Actinobacteria*. *Microbiol. Mol. Biol. Rev.* **80**, 1-43, doi:10.1128/MMBR.00019-15 (2016).

12   Chen, X. *et al.* A trehalose biosynthetic enzyme doubles as an osmotic stress sensor to regulate bacterial morphogenesis. *PLoS Genet.* **13**, e1007062, doi:10.1371/journal.pgen.1007062 (2017).

13   Alvarez, H. M. *et al.* Physiological and morphological responses of the soil bacterium *Rhodococcus opacus* strain PD630 to water stress. *FEMS Microbiol. Ecol.* **50**, 75-86, doi:10.1016/j.femsec.2004.06.002 (2004).

14   Klieneberger, E. The natural occurrence of pleuropneumonia-like organisms in apparent symbiosis with *Streptobacillus moniliformis* and other bacteria. *J Pathol Bacteriol* **40**, 93-105 (1935).

15   Leaver, M., Dominguez-Cuevas, P., Coxhead, J. M., Daniel, R. A. & Errington, J. Life without a wall or division machine in *Bacillus subtilis*. *Nature* **457**, 849-853, doi:10.1038/nature07742 (2009).

16   Frenkel, A. & Hirsch, W. Spontaneous development of L forms of Streptococci requiring secretions of other bacteria or sulphydryl compounds for normal growth. *Nature* **191**, 728-730 (1961).

617 17 Studer, P. *et al.* Proliferation of *Listeria monocytogenes* L-form cells by formation of
618   internal and external vesicles. *Nat Commun* **7**, 13631, doi:10.1038/ncomms13631
619   (2016).
620 18 Errington, J., Mickiewicz, K., Kawai, Y. & Wu, L. J. L-form bacteria, chronic
621   diseases and the origins of life. *Philosophical Transactions of the Royal Society B:*
622   *Biological Sciences* **371**, doi:10.1098/rstb.2015.0494 (2016).
623 19 Innes, C. M. J. & Allan, E. J. Induction, growth and antibiotic production of
624   *Streptomyces viridifaciens* L-form bacteria. *J. Appl. Microbiol.* **90**, 301-308 (2001).
625 20 Mercier, R., Kawai, Y. & Errington, J. Excess membrane synthesis drives a primitive
626   mode of cell proliferation. *Cell* **152**, 997-1007, doi:10.1016/j.cell.2013.01.043 (2013).
627 21 Kawai, Y. *et al.* Cell growth of wall-free L-form bacteria is limited by oxidative
628   damage. *Curr. Biol.* **25**, 1613-1618, doi:10.1016/j.cub.2015.04.031 (2015).
629 22 Mercier, R., Kawai, Y. & Errington, J. General principles for the formation and
630   proliferation of a wall-free (L-form) state in bacteria. *Elife* **3**, doi:10.7554/eLife.04629
631   (2014).
632 23 Errington, J. L-form bacteria, cell walls and the origins of life. *Open Biol* **3**, 120143,
633   doi:10.1098/rsob.120143 (2013).
634 24 Fuchino, K., Flärdh, K., Dyson, P. & Ausmees, N. Cell-biological studies of osmotic
635   shock response in *Streptomyces* spp. *J. Bacteriol.* **199**, doi:10.1128/JB.00465-16
636   (2017).
637 25 Zhu, H. *et al.* Eliciting antibiotics active against the ESKAPE pathogens in a
638   collection of actinomycetes isolated from mountain soils. *Microbiology* **160**, 1714-
639   1725, doi:10.1099/mic.0.078295-0 (2014).
640 26 Girard, G. *et al.* A novel taxonomic marker that discriminates between
641   morphologically complex actinomycetes. *Open Biol* **3**, 130073,
642   doi:10.1098/rsob.130073 (2013).
643 27 Merrick, M. J. A morphological and genetic mapping study of bald colony mutants of
644   *Streptomyces coelicolor*. *J Gen Microbiol* **96**, 299-315 (1976).
645 28 Álvarez-Álvarez, R. *et al.* A 1.8-Mb-reduced *Streptomyces clavuligerus* genome:
646   relevance for secondary metabolism and differentiation. *Appl. Microbiol. Biotechnol.*
647   **98**, 2183-2195, doi:10.1007/s00253-013-5382-z (2014).
648 29 Ramijan, K., van Wezel, G. P. & Claessen, D. Genome sequence of the filamentous
649   actinomycete *Kitasatospora viridifaciens*. *Genome Announc* **5**,
650   doi:10.1128/genomeA.01560-16 (2017).
651 30 Kempf, B. & Bremer, E. Uptake and synthesis of compatible solutes as microbial
652   stress responses to high-osmolality environments. *Arch. Microbiol.* **170**, 319-330
653   (1998).
654 31 Lebre, P. H., De Maayer, P. & Cowan, D. A. Xerotolerant bacteria: surviving through
655   a dry spell. *Nat. Rev. Microbiol.* **15**, 285-296, doi:10.1038/nrmicro.2017.16 (2017).
656 32 Maccario, L., Sanguino, L., Vogel, T. M. & Larose, C. Snow and ice ecosystems: not
657   so extreme. *Res. Microbiol.* **166**, 782-795, doi:10.1016/j.resmic.2015.09.002 (2015).
658 33 De Maayer, P., Anderson, D., Cary, C. & Cowan, D. A. Some like it cold:
659   understanding the survival strategies of psychrophiles. *EMBO Rep* **15**, 508-517,
660   doi:10.1002/embr.201338170 (2014).
661 34 Jones, S. E. *et al. Streptomyces* exploration is triggered by fungal interactions and
662   volatile signals. *Elife* **6**, doi:10.7554/eLife.21738 (2017).
663 35 Kilcher, S., Studer, P., Muessner, C., Klumpp, J. & Loessner, M. J. Cross-genus
664   rebooting of custom-made, synthetic bacteriophage genomes in L-form bacteria. *Proc*
665   *Natl Acad Sci U S A* **115**, 567-572, doi:10.1073/pnas.1714658115 (2018).

666   36   Claverys, J. P., Prudhomme, M. & Martin, B. Induction of competence regulons as a
667   general response to stress in gram-positive bacteria. *Annu. Rev. Microbiol.* **60**, 451-
668   475, doi:10.1146/annurev.micro.60.080805.142139 (2006).
669   37   Slager, J., Kjos, M., Attaiech, L. & Veening, J. W. Antibiotic-induced replication
670   stress triggers bacterial competence by increasing gene dosage near the origin. *Cell*
671   **157**, 395-406, doi:10.1016/j.cell.2014.01.068 (2014).
672   38   Holmes, N. A. *et al.* Coiled-coil protein Scy is a key component of a multiprotein
673   assembly controlling polarized growth in *Streptomyces*. *Proc Natl Acad Sci U S A*
674   **110**, E397-406, doi:10.1073/pnas.1210657110 (2013).
675   39   Kawai, Y., Mickiewicz, K. & Errington, J. Lysozyme counteracts β-Lactam
676   antibiotics by promoting the emergence of L-form bacteria. *Cell* **172**, 1038-
677   1049.e1010, doi:https://doi.org/10.1016/j.cell.2018.01.021 (2018).
678   40   Stuttard, C. Temperate phages of *Streptomyces venezuelae*: lysogeny and host
679   specificity shown by phages SV1 and SV2. *J Gen Microbiol* **128**, 115-121 (1982).
680   41   Kieser, T., Bibb, M. J., Buttner, M. J., Chater, K. F. & Hopwood, D. A. *Practical
681   Streptomyces genetics*. (The John Innes Foundation, 2000).
682   42   Schindelin, J. *et al.* Fiji: an open-source platform for biological-image analysis. *Nat.
683   Methods* **9**, 676-682, doi:10.1038/nmeth.2019 (2012).
684

685 **LEGENDS**

686 **Figure 1. High levels of sucrose affect growth and morphology of *K. viridifaciens*.** (A)

687 Growth curves of *K. viridifaciens* in LPB medium supplemented with increasing amounts of

688 sucrose. High levels of osmolytes reduce the number and size of colonies (B) in comparison

689 to media without osmolytes (C). Mycelial morphology *K. viridifaciens* grown in LPB without

690 sucrose (D) and with 0.64M of sucrose (E). Mycelium was stained with FM5-95 and SYTO-9

691 to visualize membranes and DNA, respectively. Please note the S-cells (arrowheads in E) and

692 indentations along the cylindrical part of the hypha (black arrowheads in BF panel) formed in

693 medium containing high levels of sucrose. Scale bars represent 10 mm (B, C), 10 µm (left

694 panels in D, E) and 20 µm (magnified section in D and E).

695

696 **Figure 2. Formation of S-cells is widespread in filamentous actinomycetes.** (A)

697 Morphology of S-cells released by *K. viridifaciens*, *S. venezuelae*, and a number of

698 filamentous actinomycetes from our culture collection (all referred to with the prefix MBT).

699 Cells were stained with FM5-95 (red) and SYTO-9 (green) to visualize membranes and

700 DNA, respectively. (B) Phylogenetic tree of filamentous actinomycetes based on the

701 taxonomic marker *ssgB.* Strains with the ability to form S-cells are indicated with an asterisk

702 (*). *Streptomyces* strains that are able to produce spores in liquid-grown cultures are referred

703 to as LSp (for Liquid Sporulation), while those unable to sporulate in liquid environments are

704 called NLSp (No Liquid Sporulation [26]). This classification is based on amino acid residue

705 128 in the conserved SsgB protein, which is a threonine (T) or glutamine (Q) for LSp and

706 NLSp strains, respectively. Please note that an arginine (R) is present at this position in all

707 *Kitasatospora* strains (C). Scale bars represent 5 µm

708

709 **Figure 3. S-cells represent a new cell type with the ability to switch to the mycelial**

710 **mode-of-growth.** (A) Time-lapse microscopy stills showing the extrusion of S-cells (arrows)

711 from hyphal tips. The arrow heads indicate new branches, while "S" designates the

712 germinated spore. Images were taken from Supplementary Video S1 (B) Z-stack projection

713 of filtered S-cells (taken from Supplementary Video 3). Cells were stained with Hoechst and

714 FM5-95 to visualize DNA and membranes, respectively. The intracellular membrane

715 assemblies are indicated with white arrows. (C) Transmission electron micrographs of S-cell

716 reveal the presence of agglomerates of membrane structures (white arrow) in close proximity

717 to the DNA. Contrary to filamentous cells (F, G), S-cells possess a disorganized cell surface

718 (D, E). (H) The S-cells are viable cells with the ability to form mycelial colonies on LPM

719   medium after 7 days of growth. (I) Time-lapse microscopy stills demonstrating the switch of

720   S-cells (asterisk, t=0 min) to filamentous growth. Please note that S-cells are also extruded

721   from newly-formed hyphal tips (arrowheads, t=600 min). Images were taken from

722   Supplementary Video 4. Scale bars represents 10 µm (A, B), 5 µm (magnified section in B),

723   2 µm (C), 100 nm (D, E), 20 nm (F), 50 nm (G) and 20 µm (I).

724

725   **Figure 4. S-cells switching to the mycelial mode-of-growth frequently leads to loss of the**

726   **megaplasmid KVP1**. The switch of S-cells to the mycelial mode-of-growth yields colonies

727   with different morphologies: besides grey-pigmented colonies (R1, R2), colonies are formed

728   that fail to develop efficiently, and which appear whitish or brown (R3-R5). (C) Subculturing

729   of R1 and R2 leads to the formation of grey colonies that appear similar to the wild type,

730   while subculturing of R3, R4 and R5 yield colonies that are unable to form a robust

731   sporulating aerial mycelium (brown and white colonies). Quantitative real time PCR of the

732   *infB* (C) and *allC* (D) genes using gDNA of the wild type and R3-R5 as the template. In all

733   strains, the *infB* gene located on the chromosome is amplified before the 20th cycle. However,

734   the *allC* gene, located on the KVP1 megaplasmid, is amplified in the wild type before the 20th

735   cycle, but in strains R3-R5 after the 30th cycle. (F) Quantitative comparison of the relative

736   abundance of four megaplasmid genes (*orf1*, *parA, tetR* and *allC*) and the *infB* gene (located

737   on the chromosome) between the wild type and strains R3-R5. The strong reduction in the

738   abundance of the megaplasmid genes are consistent with loss of this plasmid.

739

740   **Figure 5. Hyperosmotic stress conditions are sufficient to obtain strains that are able to**

741   **proliferate without the cell wall.** (A) Morphology of colonies of the *K. viridifaciens* wild-

742   type strain, the PenG-induced L-form strain and strains M1 and M2 on LPMA medium.

743   Please note that the wild-type strain forms compact, yellowish mycelial colonies, while the

744   other strains form mucoid green colonies. (B) Morphology of S-cells in comparison to cells

745   of the PenG-induced L-form strain and strains M1 and M2 grown for 48 hours in LPB

746   medium. Cells were stained with FM5-95 and SYTO-9 to visualize membranes and DNA,

747   respectively. Please note that the morphology of cells of strains M1 and M2 is similar to the

748   PenG-induced L-forms. The arrowheads indicate intracellular vesicles, while empty vesicles

749   are indicated with an asterisk. The inlay in M2 shows a proliferation-associated tubulation

750   event. (C-E) Frames from time-lapse microscopy show L-form-like proliferation involving

751   (C) vesiculation, (D) blebbing, and (E) membrane tubulation. (F) Formation of S-cells strains

752   upon prolonged exposure to hyperosmotic stress. Germination of spores under hyperosmotic

753   stress conditions generates germlings, which are able to extrude S-cells. These S-cells are

754   able to switch to the mycelial mode-of-growth, or sporadically acquire mutations that allow

755   them to proliferate like L-forms, which is characterized by tubulation, blebbing or

756   vesiculation. Scale bar represents 10 µm (B), 2 µm (inlay panel B) or 5 µm (C, D, E).

757

758   **Figure S1**. **High levels of salt affect growth and morphology of *K. viridifaciens*.** (A)

759   Growth curves of *K. viridifaciens* in LPB medium supplemented with different amounts of

760   NaCl. (B) S-cells (arrowheads) are evident after 96 hours of growth in the presence of 0.3

761   (middle) or 0.6 M NaCl (bottom). Mycelial morphology of *K. viridifaciens* grown in the

762   presence of 0.6 M NaCl after 48 (C), and 96 hours (D). Mycelium was stained with FM5-95

763   and SYTO-9 to visualize membranes and DNA, respectively. After 48 hours in the presence

764   of NaCl, only small aggregates of spores and germlings were visible. Pellets obtained after 96

765   hours showed an excess of membrane and hypercondensation of DNA. Scale bars represent

766   10 µm (B), or 20 µm (C-D).

767

768   **Figure S2. Comparison between different types of cell wall-deficient cells of *K.***

769   ***viridifaciens*.** (A) Morphology of freshly made protoplasts (top panels), PenG-induced L-

770   forms (middle panels) and S-cells (bottom panels). Cells were stained with the membrane dye

771   FM5-95 or fluorescent vancomycin (van^{FL}) to detect nascent PG. (B) Morphology of

772   protoplasts (top panels) and S-cells (bottom panels) grown for 48 hours in LPB. Cells were

773   stained with the membrane dye FM5-95 or wheat germ agglutinin (WGA-Oregon) to detect

774   newly synthesized PG. Scale bars represents 10 µm.

775

776   **Figure S3. Formation of S-cells is a natural adaptation in filamentous actinomycetes.**

777   (A) Microscopic analysis of strains grown for 7 days in liquid medium containing high levels

778   of osmolytes. Cells were stained with FM5-95 and SYTO-9 to visualize membranes and

779   DNA, respectively. Arrowheads indicate S-cells produced by the different strains. (B)

780   Phylogenetic tree of filamentous actinomycetes based on the 16S rDNA gene. Strains with

781   the ability to form S-cells are indicated with an asterisk (*). Scale bars represents 10 µm.

782

783   **Figure S4. The presence of abundant peptidoglycan surrounding S-cells confers**

784   **resistance to water treatment.** (A) Filtered S-cells were stained with the membrane dye

785   FM5-95 and WGA-Oregon to stain nascent peptidoglycan. The inlay shows an S-cell

786   possessing abundant cell wall material surrounding the cell surface. (B) Morphology of S-

787   cells after exposing them to water. While many cells lyse, some S-cells remain intact, which

788   invariably have abundant cell wall material associated with their cell surface (see inlay).

789   Scale bars represents 10 µm (A-B), and 5 µm (inlays).

790

791   **Figure S5. The hyperosmotic stress-induced strains M1 and M2 are cell wall-deficient**

792   **variants.** Morphology of cells of strains M1 and M2 grown for 48 hours in LPB. Cells were

793   stained with WGA-Oregon to visualize nascent PG. The scale bar represents 10 µm.

794

795   **Figure S6. Proliferation in the cell wall-deficient state leads to loss of the megaplasmid**

796   **KVPI.** Quantitative real time PCR of the *infB* (A) and *allC* (B) genes using gDNA of the

797   wild-type strain, the PenG-induced L-form strain, and strains M1 and M2. In all strains, the

798   *infB* gene located on the chromosome is amplified before the 20th cycle. However, the *allC*

799   gene, located on the KVP1 megaplasmid, is only amplified in the wild type strain, but not in

800   any of the other strains. (F) Quantitative comparison of the relative abundance of four

801   megaplasmid genes (*orf1*, *parA*, *tetR* and *allC*) and the *infB* gene (located on the

802   chromosome) between the wild-type strain, the PenG-induced L-form strain, and strains M1

803   and M2.

804

805   **Extended Data Video S1. Apical extrusion of S-cells in *K. viridifaciens*.** S-cells are

806   extruded from the hyphal tip after 425 min, coinciding with a transient arrest in tip growth.

807   After extrusion of S-cells, a new tip is formed in the apical region of the hyphae after 540

808   min, while subapically new branches become visible after 620 min. The times are indicated

809   in min. The scale bar represents 10 µm.

810

811   **Extended Data Video S2. Extrusion of S-cells from branches in *K. viridifaciens*.** S-cells

812   are extruded from the tips of branches that are formed subapically. The times are indicated in

813   min. Scale bar represents 10 µm.

814

815   **Extended Data Video S3. S-cells of *K. viridifaciens* contain DNA and inner membrane**

816   **assemblies.** Z-stack projects of S-cells isolated after 48 hours, which were stained with

817   Hoechst (blue) and FM5-95 (red) to visualize DNA and membranes, respectively. The scale

818   bar represents 10 µm.

819

820   **Extended Data Video S4. Switching of S-cells to the mycelial mode-of-growth.** Switching

821   of S-cells on solid LPMA medium yields colonies consisting of both hyphae and S-cells. The

822   times are indicated in min. The scale bar indicates 20 µm.

823

824   **Extended Data Video S5. Example of vesiculation during proliferation of strain M2.**

825   Time-lapse microscopy showing proliferation of strain M2 on media containing high levels

826   of sucrose. Please note that vesiculation is evident in some cells. The times are indicated in

827   min. The scale bar indicates 5 µm.

828

829   **Extended Data Video S6. Example of blebbing during proliferation of strain M2.** Time-

830   lapse microscopy showing proliferation of strain M2 on media containing high levels of

831   sucrose. Please note that blebbing is evident in some cells. The times are indicated in min.

832   The scale bar indicates 5 µm.

833

834   **Extended Data Video S7. Example of membrane tubulation during proliferation of**

835   **strain M2.** Time-lapse microscopy showing membrane tubulation in strain M2 during

836   proliferation on media containing high levels of sucrose. The times are indicated in min. The

837   scale bar indicates 5 µm.

Extended Data Table 1. Image analysis measurements on hyphae formed in the presence of low levels of osmolytes

Hyphae	Length (μm)	Number of branches	Branching frequency	Membrane fraction	Average nucleoid area (μm^2)
1	86,0180	1	0,01	0,10	2,53
2	90,377	3	0,03	0,09	2,01
3	72,3597	7	0,10	0,10	1,90
4	83,9838	0	0,00	0,10	3,02
5	79,0436	0	0,00	0,09	3,21
6	65,3853	1	0,02	0,17	4,18
7	80,7872	7	0,09	0,07	2,11
8	86,3086	2	0,02	0,10	3,05
9	76,4282	3	0,04	0,08	2,14
10	74,1033	2	0,03	0,12	1,71
Average	79,4795	2,6	0,03	0,10	2,59
SD	7,5857	2,5	0,03	0,03	0,77

Extended Data Table 2. Image analysis measurements on hyphae formed in the presence of high levels of osmolytes

Hyphae	length (μm)	Number of branches	Branching frequency	Membrane Fraction	Average nucleoid area (μm^2)
1	82,5308	11	0,13	0,22	1,35
2	90,9580	6	0,07	0,18	2,10
3	88,3428	8	0,09	0,16	1,82
4	60,4451	12	0,20	0,29	1,86
5	86,0180	9	0,10	0,24	2,08
6	76,7188	6	0,08	0,21	2,05
7	88,6334	6	0,07	0,22	2,34
8	53,4707	8	0,15	0,19	1,47
9	69,1631	7	0,10	0,20	2,04
10	70,3255	2	0,03	0,21	1,15
Average	76,6606	7,5	0,10	0,21	1,83
STDEVA	12,9242	2,8	0,05	0,03	0,38

Extended Data Table 3. Comparison between *K.viridifaciens* cell wall-deficient cells

Characteristic	Protoplast	L-form	S-cell
Origin	Osmoprotective conditions combined with lysozyme treatment	Osmoprotective conditions combined with prolonged exposure to lysozyme and PenG	Osmoprotective conditions
Area (μm^2)	4.01 ± 1.93	$7,06\pm5.87$	20.73 ± 11.53
Cell wall	Homogeneous regeneration. Wall material mostly associated with the cell surface	Not uniform, disordered assembly. Wall material often detached from the cell surface	Not uniform, disordered assembly. Wall material sometimes detached from the cell surface
Genotype	Wild type	Mutant	Wild-type

Extended Data Table 4. Calculated diameters (D) of S-cells released by different filamentous actinomycetes upon hyperosmotic stress. The diameters are indicated in µm.

Strain	D_{min}	D_{max}	D_{mean}	SD
K.viridifaciens	7,77	10,04	8,91	1,60
S.venezuelae	2,06	3,68	2,87	1,15
MBT13	2,62	4,49	3,56	1,32
MBT61	3,84	10,67	7,25	4,82
MBT63	2,52	5,21	3,86	1,91
MBT64	2,12	4,99	3,55	2,03
MBT66	2,56	6,78	4,67	2,99
MBT69	3,87	6,27	5,07	1,70
MBT89	2,01	6,05	4,03	2,86

Extended Data Table 5. Mutations in the hyperosmotic stress-induced S-form strain M1

Variation	Position	Type	Reference	Allele	Locus	Protein	Effect in protein
1	4456932	SNV	C	G	BOQ63_RS28320	Acetyltransferase	Leu99Val
2	4876534	SNV	T	C	BOQ63_RS30295	Valine-tRNA ligase	Val319Ala
3	3219590	SNV	C	G	NCR		
4	3133612	SNV	G	A	BOQ63_RS21920	Metal ABC transporter ATPase	Asp504Asn

SNV: Single Nucleotide Variation

Extended Data Table 6. Mutations in the hyperosmotic stress-induced S-form strain M2

Variation	Position	Type	Reference	Allele	Locus	Protein	Effect in protein
1	2164717	SNV	A	G	NCR		
2	5054842	SNV	T	G	BOQ63_RS31145	XRE family transcriptional regulator	Glu332Ala
3	6460621-6460623	Deletion	CCA	-	BOQ63_RS37840	Histidine kinase	Thr606del
4	3 133753^3133754	Insertion	-	C	BOQ63_RS21920	Metal ABC transporter ATPase	Arg553fs

SNV: Single Nucleotide Variation, del: deletion, fs: frame shift

Extended Data Table 7. Mutations in the PenG induced L-form

Variation	Position	Type	Reference	Allele	Locus	Protein	Effect in protein
1	546832	SNV	C	A	NCR		
2	3549271	SNV	G	A	BOQ63_RS23890	Lysylphosphatidylglycerol synthetase-like protein	Thr203Ile
3	3297354	SNV	C	A	BOQ63_RS22750	Undecaprenyl-diphosphate phosophatase	Leu58Met

SNV: Single Nucleotide Variation

Extended Data Table 8. Strains used in this study

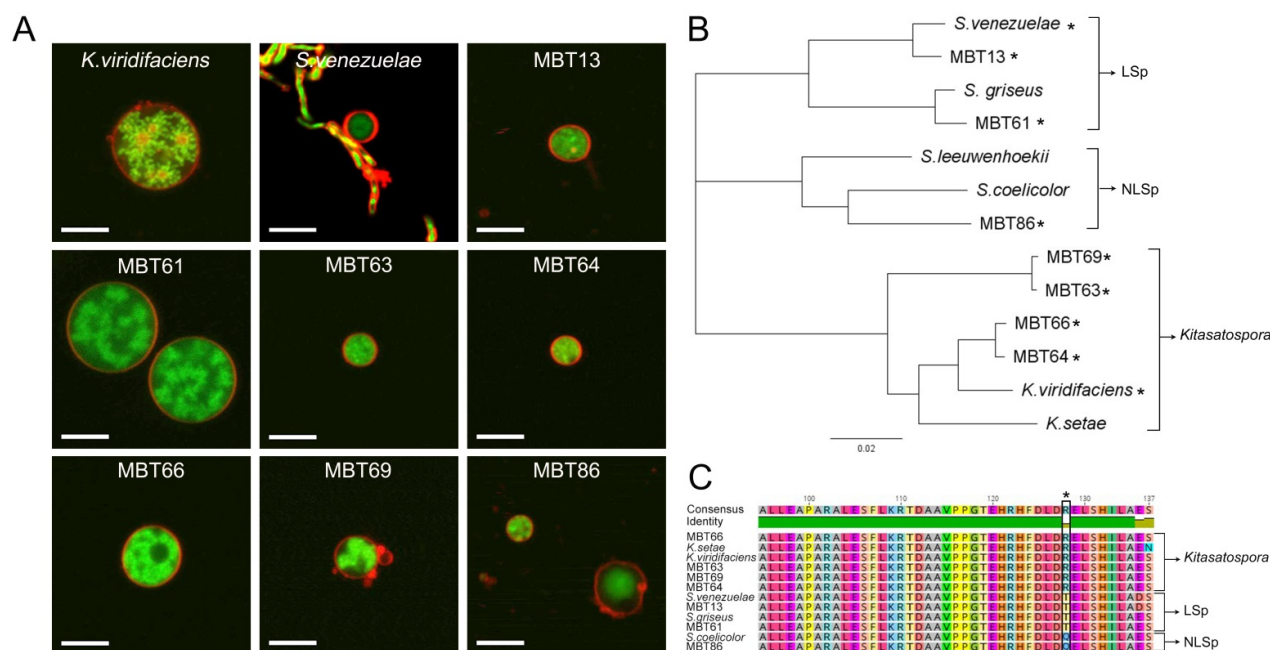| Strains	Genotype	Reference
***Streptomyces/Kitasatospora* strains**		
Streptomyces coelicolor A3(2) M145	Wild-type	Lab collection
Streptomyces lividans 1326	Wild-type	Lab collection
Streptomyces griseus	Wild-type	Lab collection
Streptomyces venezuelae DIVERSA	Wild-type	Lab collection
Kitasatospora viridifaciens DSM40239	Wild-type	DSMZ, (Ramijan et al. 2017)
Streptomyces sp. MBT13	Wild-type	Lab collection (Zhu et al. 2014)
Streptomyces sp. MBT61	Wild-type	Lab collection (Zhu et al. 2014)
Kitasatospora sp. MBT63	Wild-type	Lab collection (Girard, 2014)
Kitasatospora sp. MBT64	Wild-type	Lab collection (Zhu et al. 2014)
Kitasatospora sp. MBT66	Wild-type	Lab collection (Girard, 2014)
Kitasatospora sp. MBT69	Wild-type	Lab collection (Zhu et al. 2014)
Streptomyces sp. MBT86	Wild-type	Lab collection (Zhu et al. 2014)
***K.viridifaciens* cell wall-deficient strains**		
PenG-induced L-form	Mutant	This work
Hyperosmotic stress-induced S-form M1	Mutant	This work
Hyperosmotic stress-induced *S*-form M2	Mutant	This work

Extended Data Table 9: Primers used in this study

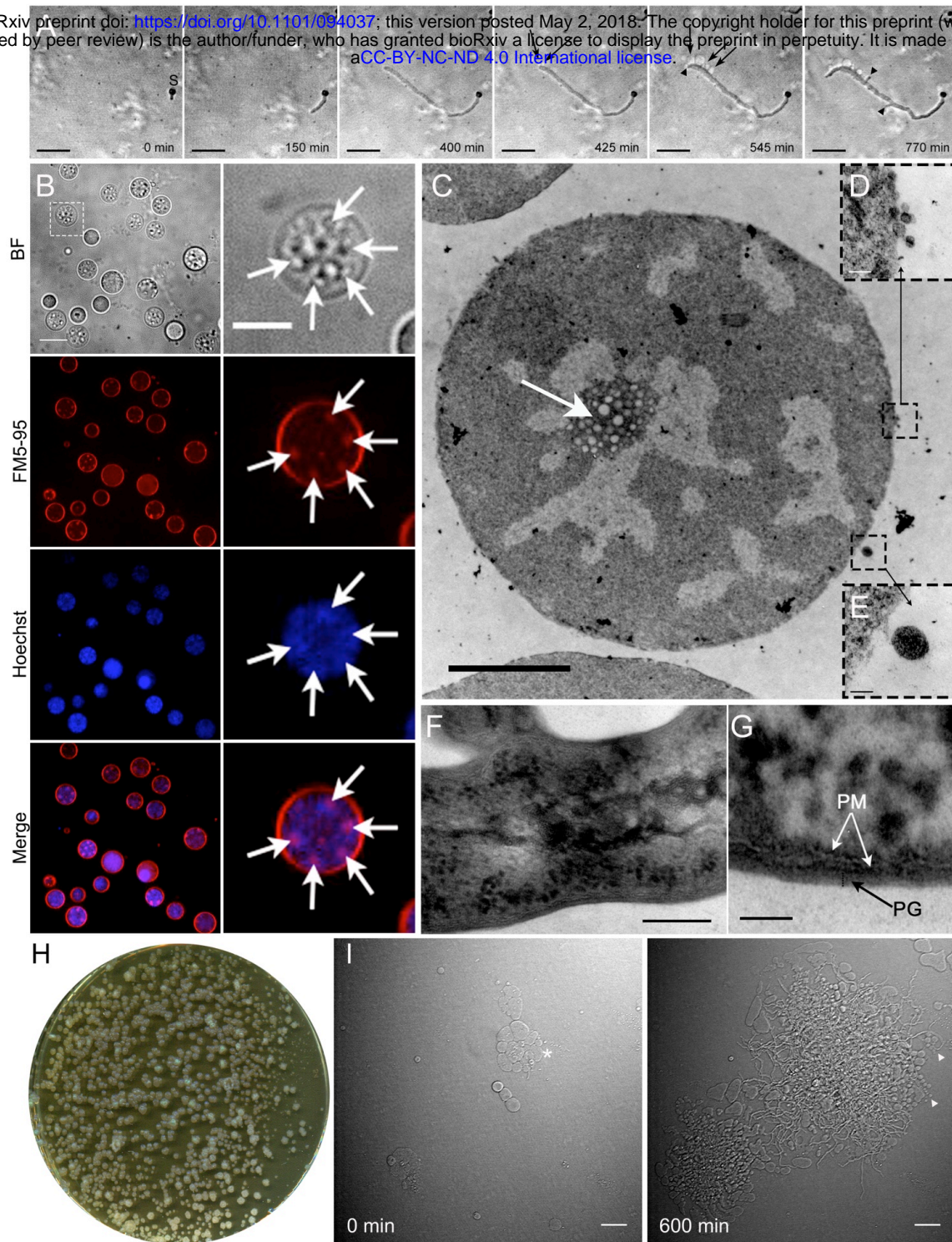| Primer	Sequence (5' – 3')
Consensus_*ssgB*-Fw	ATGAACACCACGGTCAGCTG
Consensus_s*sgB*-Rv	GCTCTCGGCCAGGATGTG
qPCR_*infB*-Fw	GTCACGTCGACCACGGTAAG
qPCR_*infB*-Rv	CACCGATGTGCTGGGTGATG
qPCR_*atpD*-Fw	TTCGGACAGCTCGTCCATAC
qPCR_*atpD*-Rv	ACATCGCGCAGAACCACTAC
qPCR_*parA*-Fw	CGGTCGTCACCCAGTACAAG
qPCR-*parA*-Rv	TAACCGAGTTCGAGGGACAG
qPCR-*Orf1*-Fw	GAGGGAGCCAATCCCGTATC
qPCR-*Orf1*-Rv	GGCTGTTGGACAGGACCATC
qPCR-*allC*-Fw	CGGCGATAGCGGAGACTAAG
qPCR-*allC*-Rv	CCACTGGTGGGACCAGAAAG
qPCR-*tetR*-Fw	TGCTCGACCAGCTGTTGAAG
qPCR-*tetR*-Rv	TGGCGAGCATGAAGTCGTAG
BOQ63_RS28320-Fw	CTAGGTCGAAGGACCGATGG
BOQ63_RS28320-Rv	CGGACGTGACGCTCTACAAC
Seq_RS28320-Rv	GAAATCGGCCAGCGGGTAAG
Seq_RS30295-Fw	CTTCAAGCGCCTGTTCGACG
Seq_RS30295-Rv	TGTCGACCCAGTCGAAGTAG
Seq_NCR-M1-Fw	CGTTGCGGATGTGGTTCTTG
Seq_NCR-M1-Rv	GTTCGCTGGCCGAGATGTTC
Seq_RS21920-Fw	TGATCGAGGCGATGCCCTTC
Seq_RS21920-Rv	CGTTCGATGTTGCCGATCAC
Seq_NCR-M2-Fw	AGAGCAGCATGCCGAGCTTG
Seq_NCR-M2-Rv	CTTCCTTGGTCGGGAAGTAG
Seq_RS31145-Fw	GTGGTGAATCCGTGCCACAG
Seq_RS31145-Rv	TGGAACGCCTACTCCATGGG
Seq_RS37840-Fw	GATCTCCACGCCGTTGAAAG
Seq_RS37840-Rv	GAGTTCGGTGGTTTCGAAGG
Seq_NCR-L-form-Fw	GTGGCTCATTCAGGACTCTC
Seq_NCR-L-form-Rv	CGCCGCTTCATCTCTGATAC
Seq_RS23890-Fw	GAGAAGATCACCGCCTTGTC
Seq_RS23890-Rv	ACAGGCACCCGCTCAACTAC
Seq_RS22750-Fw	CCGGTGACACCCGGAAATAC
Seq_RS22750-Rv	CCGGGATGGTGGAGATGATG

Figure 1. High levels of sucrose affect growth and morphology of *K. viridifaciens*. (A) Growth curves of *K. viridifaciens* in LPB medium supplemented with increasing amounts of sucrose. High levels of osmolytes reduce the number and size of colonies (B) in comparison to media without osmolytes (C). Mycelial morphology *K. viridifaciens* grown in LPB without sucrose (D) and with 0.64M of sucrose (E). Mycelium was stained with FM5-95 and SYTO-9 to visualize membranes and DNA, respectively. Please note the S-cells (white arrowheads in E) and indentations along the cylindrical part of the hypha (black arrowheads in BF section) formed in medium containing high levels of sucrose. Scale bars represent 10 mm (B, C), 10 μm (left panels in D, E) and 20 μm (magnified section in D and E).
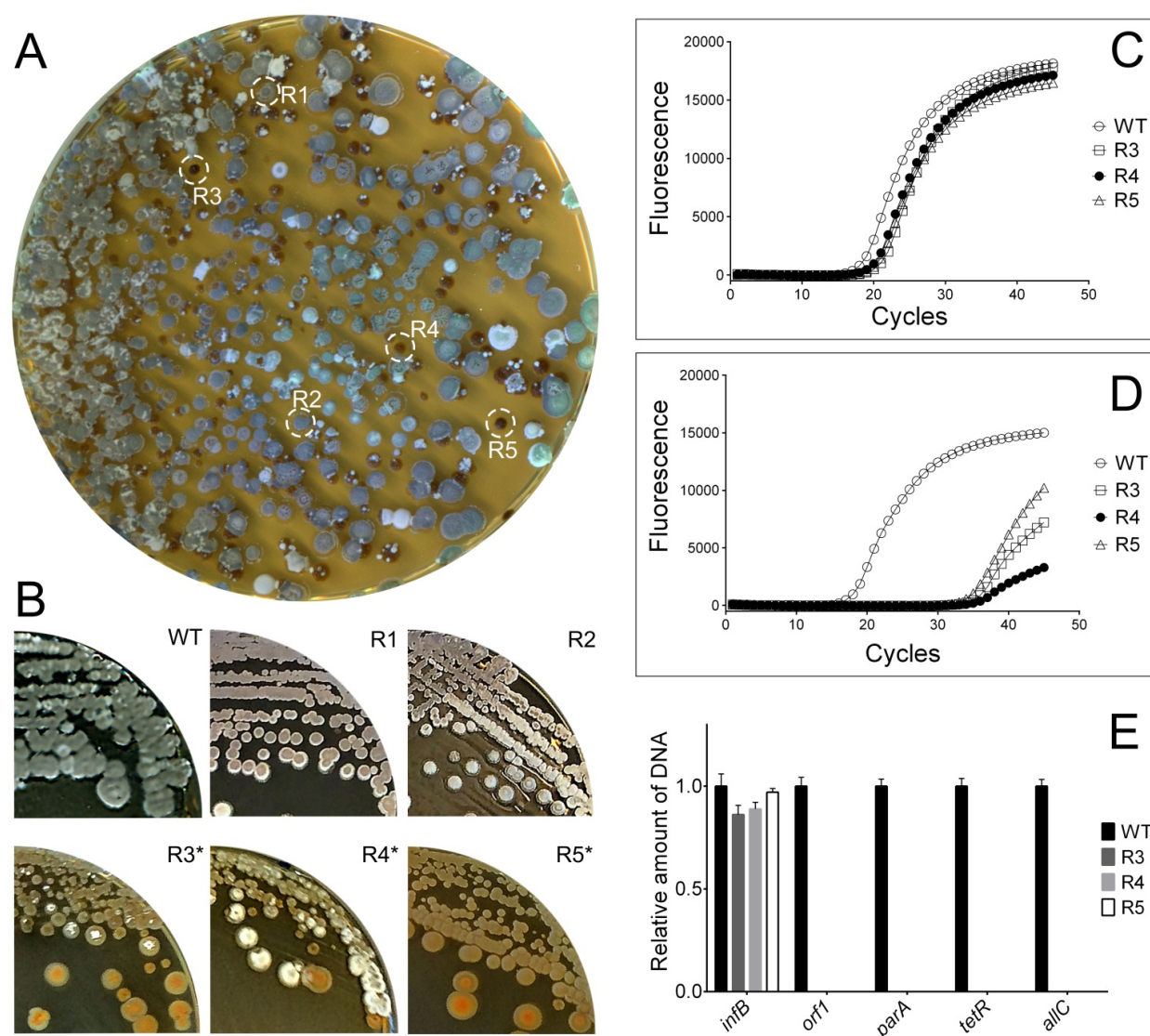
Figure 2. Formation of S-cells is widespread in filamentous actinomycetes. (A) Morphology of S-cells released by *K. viridifaciens*, *S. venezuelae*, and a number of filamentous actinomycetes from our culture collection (all referred to with the prefix MBT). Cells were stained with FM5-95 (red) and SYTO-9 (green) to visualize membranes and DNA, respectively. (B) Phylogenetic tree of filamentous actinomycetes based on the taxonomic marker *ssgB*. Strains with the ability to form S-cells are indicated with an asterisk (*). *Streptomyces* strains that are able to produce spores in liquid-grown cultures are referred to as LSp (for Liquid Sporulation), while those unable to sporulate in liquid environments are called NLSp (No Liquid Sporulation [26]). This classification is based on amino acid residue 128 in the conserved SsgB protein, which is a threonine (T) or glutamine (Q) for LSp and NLSp strains, respectively. Please note that an arginine (R) is present at this position in all *Kitasatospora* strains (C). Scale bars represent 5 µm
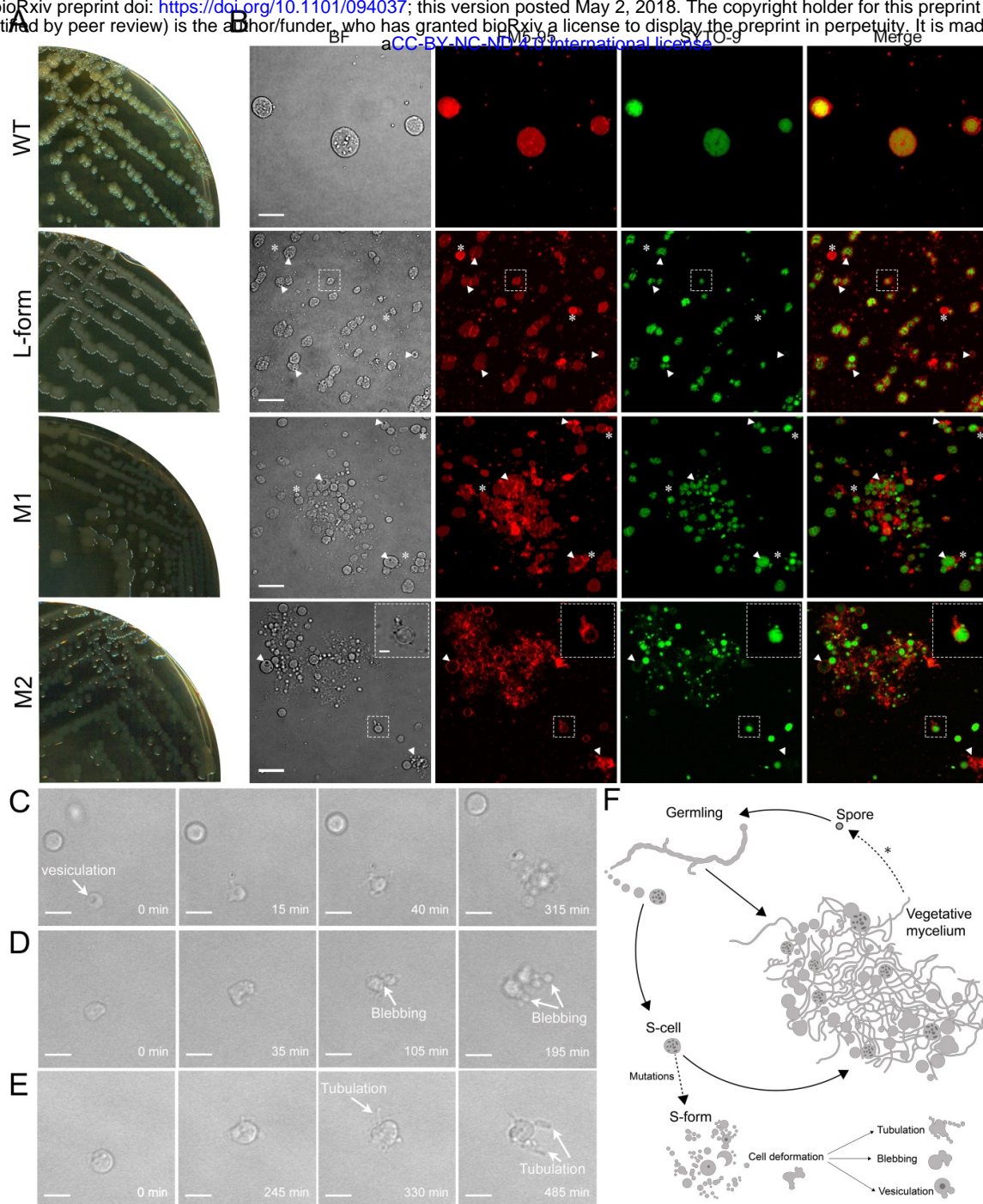
Figure 3. S-cells represent a new cell type with the ability to switch to the mycelial mode-of-growth.
(A) Time-lapse microscopy stills showing the extrusion of S-cells (arrows) from hyphal tips. The arrow heads indicate new branches, while "S" designates the germinated spore. Images were taken from Supplementary Video S1 (B) Z-stack projection of filtered S-cells (taken from Supplementary Video 3). Cells were stained with Hoechst and FM5-95 to visualize DNA and membranes, respectively. The intracellular membrane assemblies are indicated with white arrows. (C) Transmission electron micrographs of S-cell reveal the presence of agglomerates of membrane structures (white arrow) in close proximity to the DNA. Contrary to filamentous cells (F, G), S-cells possess a disorganized cell surface (D, E). (H) The S-cells are viable cells with the ability to form mycelial colonies on LPM medium after 7 days of growth. (I) Time-lapse microscopy stills demonstrating the switch of S-cells (asterisk, t=0 min) to filamentous growth. Please note that S-cells are also extruded from newly-formed hyphal tips (arrowheads, t=600 min). Images were taken from Supplementary Video 4. Scale bars represents 10 μm (A, B), 5 μm (magnified section in B), 2 μm (C), 100 nm (D, E), 20 nm (F), 50 nm (G) and 20 μm (I).

Figure 4. S-cells switching to the mycelial mode-of-growth frequently leads to loss of the megaplasmid KVP1. The switch of S-cells to the mycelial mode-of-growth yields colonies with different morphologies: besides grey-pigmented colonies (R1, R2), colonies are formed that fail to develop efficiently, and which appear whitish or brown (R3-R5). (C) Subculturing of R1 and R2 leads to the formation of grey colonies that appear similar to the wild type, while subculturing of R3, R4 and R5 yield colonies that are unable to form a robust sporulating aerial mycelium (brown and white colonies). Quantitative real time PCR of the *infB* (C) and *allC* (D) genes using gDNA of the wild type and R3-R5 as the template. In all strains, the *infB* gene located on the chromosome is amplified before the 20th cycle. However, the *allC* gene, located on the KVP1 megaplasmid, is amplified in the wild type before the 20th cycle, but in strains R3-R5 after the 30th cycle. (F) Quantitative comparison of the relative abundance of four megaplasmid genes (*orf1*, *parA, tetR* and *allC*) and the *infB* gene (located on the chromosome) between the wild type and strains R3-R5. The strong reduction in the abundance of the megaplasmid genes are consistent with loss of this plasmid.

Figure 5 . Hyperosmotic stress conditions are sufficient to isolate strains that are able to proliferate without the cell wall. (A) Morphology of colonies of the *K. viridifaciens* wild-type strain, the PenG-induced L-form strain and strains M1 and M2 on LPMA medium. Please note that the wild-type strain forms compact, yellowish mycelial colonies, while the other strains form mucoid green colonies. (B) Morphology of S-cells in comparison to cells of the PenG-induced L-form strain and strains M1 and M2 grown for 48 hours in LPB medium. Cells were stained with FM5-95 and SYTO-9 to visualize membranes and DNA, respectively. Please note that the morphology of cells of strains M1 and M2 is similar to the PenG-induced L-forms. The arrowheads indicate intracellular vesicles, while empty vesicles are indicated with an asterisk. The inlay in M2 shows a proliferation-associated tubulation event. (C-E) Frames from time-lapse microscopy show L-form-like proliferation involving (C) vesiculation, (D) blebbing, and (E) membrane tubulation. (F) Formation of S-cells strains upon prolonged exposure to hyperosmotic stress. Germination of spores under hyperosmotic stress conditions generates germlings, which are able to extrude S-cells. These S-cells are able to switch to the mycelial mode-of-growth, or sporadically acquire mutations that allow them to proliferate like L-forms, which is characterized by tubulation, blebbing or vesiculation. Scale bar represents 10 μm (B), 2 μm (inlay panel B) or 5 μm (C, D, E).